



Silver Nanoparticle Synthesized with Fenugreek Leaves Is Biologically Potent than Chemically Synthesized Nanoparticle

Kunal Kishore¹ · Pooja Prasad¹ · Nandakumar Selvasudha¹ · Saranga Rajesh¹ · Hannah R. Vasanthi¹

Accepted: 11 August 2023 / Published online: 10 September 2023

© The Author(s), under exclusive licence to Springer Science+Business Media, LLC, part of Springer Nature 2023

Abstract

Purpose Silver nanoparticles have been found to exhibit various bioactivities like antibacterial, anticancer, antifungal, and enzyme-mimicking properties and can be synthesized via chemical and biological methods.

Aim This study compares the significant characteristics of chemically and biologically synthesized silver nanoparticles with sodium borohydride and *Trigonella foenum-graecum* leaf extract as reducing and stabilizing agents, respectively.

Methods U.V. spectroscopy, FTIR (Fourier transform infrared) spectroscopy, DSC-TGA (Differential scanning calorimetry-Thermalgravimetric analysis), XPS (X-ray photoelectron spectrometer), and SEM (Scanning electron microscopy) were employed to characterize the nanoparticles. The antioxidant activity via FRAP assay, the nanoparticles' cytotoxicity, and wound healing ability using MTT and scratch assay were performed.

Results The absorption maxima were observed at 425 nm for green synthesized (GNP) and 390 nm for chemically synthesized silver nanoparticles (CNP). FTIR assignment and diffraction peaks at respective 2θ values confirmed the formation of AgNPs. The peak at 978°C in the thermogram proved the presence of silver in the biological method, and the first weight loss (42.48%) at 324.51°C for CNP exemplified the decomposition. The lower concentration of silver evidenced by XPS in GNP will benefit the toxicity-free biological effects induced by AgNPs. The presence of spherical-shaped GNP with better cell migration confirms faster wound healing with negligible toxicity compared to the multivariate-shaped CNP.

Conclusion Although the chemically synthesized silver nanoparticle exhibited good antioxidant activity, the biogenic nanoparticle showed better antimicrobial and wound-healing potential with lesser cytotoxicity on fibroblast cells relating to the size and shape of the nanoparticles synthesized. Therefore, further studies on formulations using biogenic silver nanoparticles are worth pondering.

Keywords Green synthesis · Chemically synthesis · Silver nanoparticle · Fenugreek · Scratch assay

Introduction

Nanotechnology is the most prominent sought-after domain of research in material science, which involves material dimensions on the nanometer scale compared to their macro-counterparts [1]. It is concerned with designing, producing, and manipulating particle structures ranging in size from 1 to 100 nm [2]. The nanoparticles' unique physical and chemical properties have increased scientists' interest and curiosity to develop new nanoparticle synthesis methods [3, 4]. Depending on their size, shape, and morphology, nanostructures offer a variety of uses due to their novel or improved qualities [5]. Nanoparticles have found their utility in different fields, namely in agriculture, cosmetics, medical, pharmaceutical, and chemical industries. Various metals such as iron, zinc, platinum, gold, and silver are used in preparing nanoparticles. This paper emphasizes the comparison

✉ Hannah R. Vasanthi
hrvasanthi@gmail.com; hannah.dbt@pondiuni.edu.in

Kunal Kishore
kunal.raj318@pondiuni.ac.in

Pooja Prasad
poojapdiwakaran@gmail.com

Nandakumar Selvasudha
nkselvasudha@gmail.com

Saranga Rajesh
sarangarajesh@pondiuni.ac.in

¹ Natural Products Research Laboratory, Department of Biotechnology, Pondicherry University, 605014 Kalapet, Puducherry, India

of silver nanoparticles synthesized by two methods because, since ancient times, silver has been employed in medicine as they are found to exhibit antibacterial, anticancer, antifungal, and enzyme-mimicking properties.

Either physical, chemical, or biological methods can synthesize metal nanoparticles. In the chemical manufacturing process, the chemicals used for the synthesis might be absorbed in the outer region, leading to harmful effects. Many factors, such as surface charge, shape, size, and preparation techniques, determine the cytotoxicity of silver nanoparticles used for medical purposes. It also depends on the cells with abnormal metabolism and morphology, like cancer cells. Biological methods of fabricating nanoparticles employ enzymes, microbes, fungi, and plants as capping or encapsulating agents and are environmentally acceptable choices to physical/chemical methodologies. Compared to nanoparticles generated by chemicals, nanoparticles synthesized using plant extracts have gained substantial importance owing to their cost effectiveness, stability, ease of availability and processing, and free from toxic chemicals.

Several plant products have been used to create a wide range of metal nanoparticles [6–9]. Fenugreek (*Trigonella foenum-graecum*) leaves have been used as bio-reducing and capping agents in silver nanoparticle manufacturing. The herb fenugreek (*T. foenum-graecum*) is commonly found in Mediterranean regions and used in many health ailments in many parts of the globe. Vitamins like ascorbic acid, vitamin B3, and minerals like potassium, proteins, and diosgenin are all found in fenugreek seeds. Fenugreek has also exhibited pharmacological activities like anti-inflammatory, anticancer, antimicrobial, antidiabetic, and antioxidant activities [10].

Fenugreek leaves possess a significant quantity of bioactive components such as polyphenols, flavonoids, and some glycosides, which reduce silver ions to silver nanoparticles and convert the surface of silver from positive to neutral or negative charge, which influences its biological properties significantly. Herein, we compare the antioxidant, antibacterial, and wound-healing properties of the AgNP synthesized by chemical and biological methods.

Materials and Methods

Fenugreek leaves were purchased from the local market in Puducherry. All chemicals, reagents, media, and analytical-grade solvents were procured from HiMedia.

Preparation of Silver Nanoparticles

Green Synthesis of Silver Nanoparticles by Reduction Method (GNP)

The fenugreek leaves were washed with water to eliminate specks of dirt and followed with distilled water 2–3 times.

The leaves were dried for some time by blotting the water on a filter paper. Twenty grams of leaves were weighed and mixed with 150 ml Millipore water, heated up to 80°C for 40 min to 1 h, and then incubated for 30 mins. The solution was centrifuged for 30 mins at room temperature after incubation. The supernatant obtained was filtered through a Whatman filter paper No. 1, and the same was used as the reducing agent.

Biogenic silver nanoparticles were prepared by pouring 10 ml of the prepared fenugreek leaf extract into a 100 ml silver nitrate (1 mM) (1:10) solution and stirred at 500 rpm using a magnetic stirrer. The color of the sample gradually changed after 15 mins of stirring, suggesting the formation of silver nanoparticles. Within an hour, the synthesized nanoparticles changed from colorless to pale yellow to brownish to dark brown. The Ag⁺ ions were reduced to nanosilver probably by the bioactive compounds such as flavonoids or polyphenols found in the leaves extract. Subsequently, the solution was centrifuged at ambient temperature for 30 mins at 11,000 rpm to isolate the pellet by discarding the supernatant. The pellet was rinsed with water, dried, and subjected to various techniques to characterize the biogenic silver nanoparticles (GNP).

Chemical Synthesis of Silver Nanoparticles by Reduction Method (CNP)

1 mM silver nitrate was prepared by weighing 51 mg and dissolving it in 300 ml of distilled water. Simultaneously, 30 ml of 0.002 M sodium borohydride (NaBH₄) was added to an Erlenmeyer flask submerged in an ice bath and stirred with a magnetic stirrer for around 20 min. At around one drop per second, 2 ml of 0.001 M silver nitrate (AgNO₃) was mixed with the swirling NaBH₄ solution. Stirring was halted as soon as the AgNO₃ addition was completed. The reduction of silver ions resulted in the formation of silver nanoparticles in the aqueous media. As the nanoparticles aggregated, a few drops of 1.5 M sodium chloride (NaCl) solution turned the suspension deeper yellow which was noted at 386 nm, and then turned to a gray color. The solution was further centrifuged for 30 mins at 11,000 rpm at ambient conditions to obtain the silver nanoparticles (CNP).

In Vitro Characterization of Green (GNP) and Chemically (CNP) Synthesized Silver Nanoparticles

Ultraviolet-visible Spectroscopy

The absorption spectra were determined using a UV-2700 spectrophotometer (Shimadzu, Japan) with 1.0 cm quartz cells. The samples were put into a UV transparent quartz cuvette at 25 °C and scanned between 300 and 800 nm.

Spectrofluorometric Analysis

The emission spectra of AgNPs solutions in water were obtained using a spectrofluorometer (Perkin Elmer). The highest fluorescence intensity was attained at optimal excitation wavelengths 314 and 269 nm. A cuvette filled with 4.0 ml of sample solutions was used to obtain and analyze the fluorescence spectra.

Fourier Transform Infrared Spectroscopy (FTIR)

FTIR spectra were obtained for all the samples using the KBr pellet method in Jasco FT/IR 6300 at a frequency range of 4000–400 cm^{-1} .

X-Ray Diffractogram

In order to measure the X-ray diffraction (XRD) patterns of the biogenic and chemically synthesized silver nanoparticles, XRD equipment operating at 45 kV voltage and 40 mA current were used with a Cu-K radiation source. The existence, crystallinity, and grain size of silver nanoparticles were confirmed using the XRD analysis.

Particle Size Analysis

Using XRD Data by Scherrer's Equation Method The particle size of nanoparticles can be obtained indirectly by substituting XRD data in the following formula $D = (k\lambda/\beta \cos \theta)$, where D denotes the size of an average crystallite, and β denotes the line broadening in radians (full width at half maximum of the peak in radians). X-ray wavelength is expressed as λ , and θ is Bragg's angle. K is constant (geometric factor = 0.94).

Using Zetasizer The particle size of the nanoparticles was determined using a particle size analyzer (Malvern Zetasizer, NanoZS). The sample was dispersed in water, taken in the disposable glass cuvette and analyzed.

Thermal Analysis

DSC-TGA was performed with a DSC–8000 differential scanning calorimeter (Perkin Elmer, USA). The samples were compressed in a typical aluminum pan, and DSC thermograms from 25 to 900°C were taken at a scan rate of 10°C/min while nitrogen was continuously purged at a rate of 20 ml/min.

X-Ray Photoelectron Spectrometer (XPS)

With the 1253.6 eV, pass energy of 20 eV and 0.05 eV steps, 10–10 torr pressure, the non-monochromated Mg K α , X-ray

photoemission spectroscopy was used for obtaining the spectra of samples. A few drops of the samples were used over pyrolytic graphite and dried.

Scanning Electron Microscope

The samples were gold coated, dried, and subjected to SEM analysis (SU1510 model; Hitachi Ltd., Tokyo, Japan), and the microphotographs were observed for their morphological characteristics.

Antioxidant Potential of Synthesized Nanoparticles by Ferric Reducing Antioxidant Power (FRAP) Assay

FRAP reagent was freshly prepared by combining 50 ml of 0.3 mol/L acetate buffer (CH_3COOH : CH_3COONa), pH 3.6. The solution was spiked with 5 ml of 10 mmol/L 2, 4, 6-tripyridyl-triazine (TPTZ) in 0.04 mol/L HCl and 5 ml of 0.02 mol/L $\text{FeCl}_3 \cdot 6\text{H}_2\text{O}$ (10: 5: 5). The test solution comprised 1.0 ml with distilled water and different concentrations of fenugreek leaf extract (5–50 mg/ml). The FRAP reagent was warmed to 37°C. The reaction mixture comprises 390 μl of FRAP and 10 μl of test solution. After thoroughly mixing, the reaction mixture was incubated in the dark for 30 mins. At 593 nm, the absorbance was measured. Known concentrations of $\text{FeSO}_4 \cdot 7\text{H}_2\text{O}$ were used to create a standard calibration curve. Ascorbic acid served as the reference sample, expressing antioxidant activity in ascorbic acid equivalents. A total of 10 μl of distilled water and 390 μl of FRAP were taken as blank. All tests were carried out in triplicates, and the reducing power of the test material was calculated as follows:

$$\text{Relative \% of reducing power} = \frac{(\text{Absorbance of control} - \text{Absorbance of sample})}{(\text{Absorbance of control})} \times 100$$

Antibacterial Potential by Disc Diffusion Assay

The antibacterial activity of both GNP and CNP was evaluated using gram-negative organisms, namely *Escherichia coli*, *Pseudomonas aeruginosa*, *Acetobacter baumannii*, and gram-positive bacteria *Staphylococcus aureus*. The selected pathogens were inoculated in 50 ml nutrient broth and were incubated for 24 h at 37°C. Bacterial strains were streaked on Müller-Hinton (M.H.) agar plates after being cultured overnight in the M.H. broth medium. Bacteria were allowed to develop a confluent lawn of cells on the surface of the plate. Paper discs (6 mm diameter) were sterilized and dipped in sample solutions (200 mg/ml). Under sterile circumstances, the GNP and CNP discs were air-dried and deposited on the seeded top layer of the M.H. agar plates.

The plates were then incubated at 37°C for 24 h before being checked for inhibition zones [11].

Cell Viability and Cell Proliferation Studies

Culturing of L929 Fibroblast Cells

The prepared silver nanoparticles were planned to prepare wound-dressing materials. Therefore, the L929 fibroblast cells obtained from NCCS, Pune, were used for identifying the cytotoxicity by MTT assay and wound healing studies by scratch assay. The fibroblast cells were grown in Dulbecco's Modified Eagle Medium (DMEM) in a 5% CO₂ incubator at 37°C. The cells were subcultured using Trypsin–EDTA solution and used for subsequent studies once they reached 80% confluence.

MTT Assay

The MTT assay was used to determine the cytotoxicity of the chemically and biologically synthesized AgNP against fibroblast cells. L929 fibroblast cells were seeded on a 24h cell culture plate and cultured for 24 h at 37 °C in a 5% CO₂ incubator. In order to evaluate cell viability in L929 cell lines, the MTT test (3-(4, 5-dimethylthiazol-2-yl)-2, 5-diphenyltetrazolium bromide) was utilized. Cell cultures were cultured for 2 h in culture media alone as a control (untreated cells) for measuring cell viability. The stock solution of synthesized AgNPs was made in 1 ml PBS, and GNP and CNP were checked for cytotoxicity at various doses ranging from 2–20 µM. A total of 100 µl of MTT solution was added to each well along with the medium and then incubated for 4 h at 37°C in a CO₂ incubator. In order to dissolve the formazan crystals, 200 µl aliquots of DMSO were added to each well after the MTT solution was removed, followed by 10 mins of incubation at 37°C. The treatments were carried out in triplicates, and at 570 nm, optical densities were measured spectrophotometrically, and the cell viability was calculated accordingly.

Scratch Assay

Scratch wound assay is a simple two-dimensional technique to study cell migration in vitro. Before treating the cells with AgNPs, the fibroblast cells were plated in a 6-well culture plate until they were 70–80% confluent as a monolayer to identify the wound-healing potential of the silver nanoparticles by scratch assay. Based on the IC₅₀ values obtained in the MTT assay, three concentrations (5, 10, and 20 µM) of the two synthesized silver nanoparticles (GNP and CNP) were prepared in 1 ml PBS. A 200-µl pipette tip vertically introduced the scratch to the monolayer cells. All photos were acquired using an inverted microscope (Q imaging, Olympus CKX53)

equipment at the appropriate time points. Each condition was evaluated in triplicates.

Results and Discussion

With recent advancements in nanobiotechnology, the use of silver nanoparticles in nanomedicine and biomedical applications has substantially increased [12]. Herein, we compared the quality characteristics and the bioactivity of silver nanoparticles synthesized using plant extract and chemical reduction methods. It is interesting to note that there is a substantial difference in the size, shape, and bioactivities exhibited by the CNP and GNP silver nanostructures, which are discussed below.

Preparation of Silver Nanoparticles by Chemical Reduction and Green Synthesis Method

Synthesis of nanoparticles for various applications has brought newer methods with better compliance. In the present study, the formulation at the end of the preparation turned brown, indicating silver ion reduction into silver nanoparticles. The color transformation was because of the absorption of the light wave at a specific wavelength. The excitation of metal nanoparticles causes rapid electron movement, as valence and conduction bands lie very close to each other in metals leading to the surface plasmon effect [SPR] of the absorption band. The resonance between a group of electrons in the silver nanoparticles and the light wave is the reason for this SPR effect [13]. The light wave induces the polarization of AgNPs electrons, and the light wave becomes resonant with electron movement leading to the absorption at a specific wavelength confirming the formation of nanoparticles.

Characterization of Synthesized Silver Nanoparticles

Ultraviolet-visible (UV-vis) Spectroscopy Confirming the Formation of Silver Nanoparticles

The absorption maxima were observed at 425 nm for green synthesized and 390 nm for chemically synthesized silver nanoparticles confirming that chemically synthesized nanoparticles are smaller than green synthesized nanoparticles. The wide band in the UV region is noted as a result of the inter-band transition of the silver nanoparticles, and the elongated tail in the visible red area represents the presence of polydispersed nanoparticles. The absorption peak between 380 and 470 nm is optimal for silver nanoparticles. Generally smaller sized particles are absorbed at lower wavelengths [14]. Likewise, silver nanoparticles synthesized by Pulse Laser Ablation was reported to possess a size of 407 nm [15]. Similarly, silver nanoparticles synthesized using sodium borohydride showed a size of about 400 nm [16]. Green synthesis of silver nanoparticles using

Hagenia Abyssinica plant leaf extract was reported with the absorption maximum of AgNPs at 400–430 nm [17]. It is impressive to note that fenugreek seed-catalyzed silver nanoparticles by Alwhibi and coworkers [18] correlates to the absorption maximum as in our current study. Accordingly, all the above studies support the rightness of the silver nanoparticles prepared by green and chemical synthesis (Fig. 1).

Spectrofluorometry for the Confirmation of Silver Nanoparticles

The silver nanoparticles generally have peaks between 450–490 nm in the emission spectra when excited at 293–314 nm. The spectral data obtained showed a hypsochromic shift (blue shift) for chemically synthesized AgNP. Conversely, a bathochromic shift (red shift) was noted for the green synthesized silver nanoparticles. Only one peak at 552 nm was detected in the green synthesized (GNP) silver nanoparticles (Fig. 2A). In contrast, two emission peaks at 337 and 411 nm were observed in the spectra of chemically synthesized (CNP) silver nanoparticles (Fig. 2B).

In the case of green synthesized nanoparticles, the shift towards a longer wavelength was detected due to the electron stimulus to the lower energy level. The electrons are emitted at extended wavelengths during the relaxation process [19]. The size of synthesized nanoparticles was indirectly revealed from the emission spectrum. Accordingly, the chemically synthesized nanoparticles are expected to have a smaller size when compared to the green synthesized ones. As the chemically synthesized nanoparticles are smaller than the GNPs, more free electrons are expected to contribute to intense peaks. However, in the green synthesized silver nanoparticles, the silver ion is proposed to bind with phytochemicals in the leaf extract, probably contributing fewer free electrons, resulting in less intense peaks and large-sized particles.

Fourier Transform Infrared Spectroscopy (FTIR) of Silver Nanoparticles

FTIR spectrum of AgNPs (Fig. 3) synthesized from fenugreek leaves shows the presence of –O–H, COOH, and NO groups. As the fenugreek leaves consist of polyphenols such as quercetin and naringenin [20] in high quantity, the spectra confirm the capping of polyphenol or other phytochemicals such as 4-hydroxy isoleucine [21] around AgNPs. The spectrum of the green synthesized nanoparticles showed peaks at 3436 cm^{-1} for O–H stretching, 1639 cm^{-1} for C–N vibration, 1384 cm^{-1} , and 1048 cm^{-1} corresponding to N–H and –C=C stretching vibration of primary/secondary amides and amine, respectively. The peaks assigned to 825 cm^{-1} and 777 cm^{-1} were attributed to –O–H bending. Peak at 1106 cm^{-1} corresponds to –C–O stretching vibration. A total of 3390 cm^{-1} attributed for –OH stretching vibration of carbohydrates and polyphenols in fenugreek leaves which encapsulate the green synthesized silver nanoparticles. As these functional groups are bonded with the silver nanoparticles, the weak signals were observed. A study by Alwhibi et al. (2018) [18] and Rizwana et al. (2021) [14] confirmed the FTIR assignment of silver nanoparticles prepared by green synthesis, and our results are congruent with these studies.

In the case of silver nanoparticles (CNP) synthesized by the chemical reduction method (Fig. 3), the peaks in 3390 cm^{-1} were due to the O–H stretching of compounds used for the reduction process. The peaks 1634 cm^{-1} correspond to C–N stretch vibration; 1385 cm^{-1} and 1106 cm^{-1} relate to primary and secondary amides of N–H and –C–N stretching vibration of amines. The peak at 755 cm^{-1} was allotted to O–H bending (H-bonded). This FTIR assignment agrees with the FTIR spectrum of silver nanoparticles (chemical reduction method) reported by Thiruvengadam et al., 2020 [22].

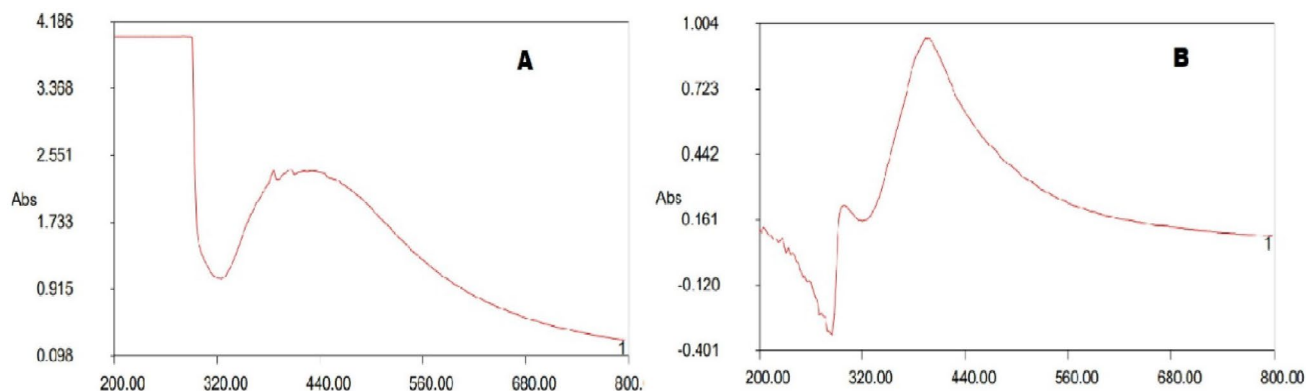


Fig. 1 Comparative UV–visible spectra of green and chemically synthesized silver nanoparticles. **A** GNP. **B** CNP

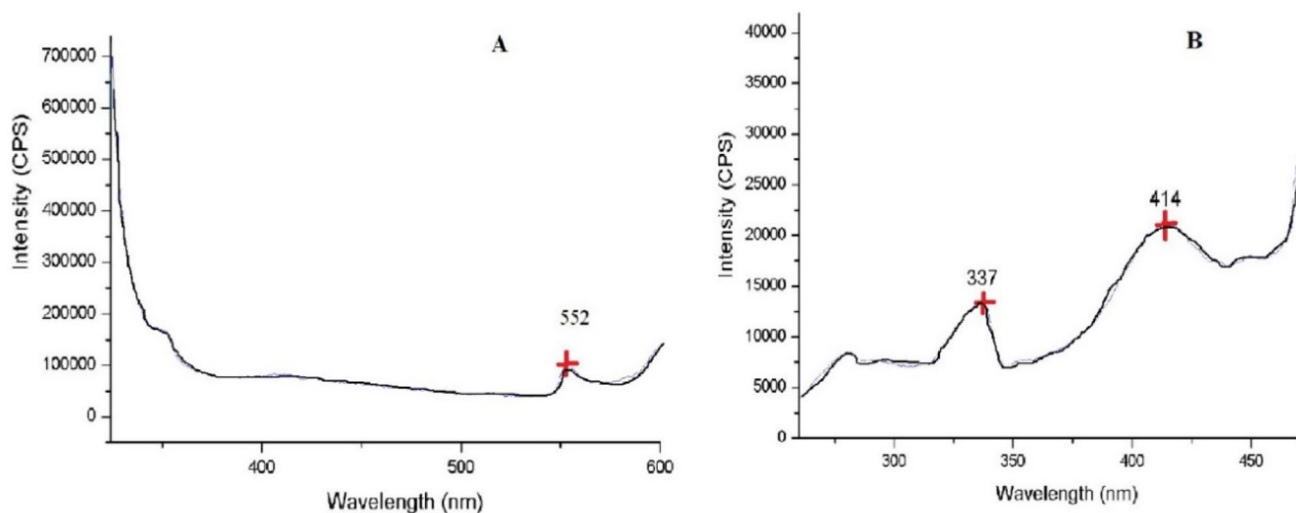


Fig. 2 Comparative fluorescence spectra of green and chemically synthesized silver nanoparticles. **A** GNP. **B** CNP

X-Ray Diffraction Analysis of Silver Nanoparticles

The X-ray diffraction peaks of the silver nanoparticles synthesized by green and chemical synthesis are shown in Fig. 4, respectively. Between green and chemical-synthesized silver nanoparticles, green synthesized AgNPs showed various diffraction peaks while chemical synthesized AgNPs exhibited very few peaks representing more crystallinity of green synthesized nanoparticles. Diffraction peaks were observed at $2\theta = 27.24^\circ, 31.69^\circ, 45.68^\circ, 54.32^\circ, 56.93^\circ, 66.97^\circ, 76.34^\circ$ for green synthesized and at $37.59^\circ, 43.78^\circ, 77.02^\circ$ for chemically synthesized nanoparticles. Ghoshal and M. Singh et al. (2022) reported four diffraction peaks at $2\theta = 38.1^\circ, 44.67^\circ, 65.02^\circ, 78.13^\circ$ for silver nanoparticles obtained from fenugreek leaves, which corresponds to (1 1 1), (2 0 0), (2 2 0), and (3 1 1) lattice planes, respectively [23]. The authors added a point that these peaks were the characteristics of a face-centered cubic structure of metallic silver, and the peak corresponding to the (1 1 1) plane was

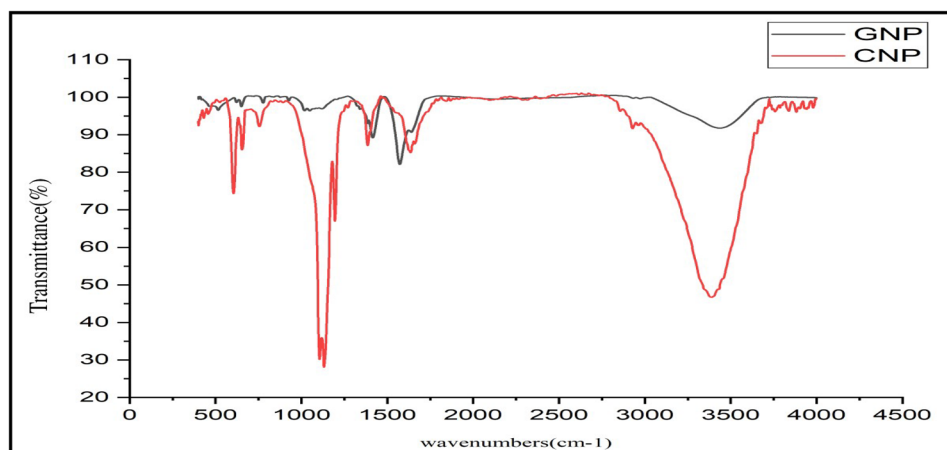
the highest. The results of the current study were similar to this reported study, and the peak corresponds to 31.69° and 37.59° were the highest for green and chemically synthesized AgNPs, respectively.

Particle Size Analysis

Using XRD Data Particle size plays a vital role in the bioactivity of a nanoparticle. Using Sherrer's equation, the particle size was indirectly calculated, resulting in 19 nm for chemically synthesized nanoparticles and 26 nm for green synthesized nanoparticles.

Using Zetasizer The particle size of green and chemically synthesized nanoparticles was analyzed by the direct method using a zeta sizer (Fig. 5). The size was within 50 nm (Z average for GNP- 30.71 ± 3.4 and CNP- 46.37 ± 5.9) and was found to be compromised with the indirect analysis method.

Fig. 3 Comparative Fourier transform infrared spectroscopy (FTIR) of silver nanoparticles



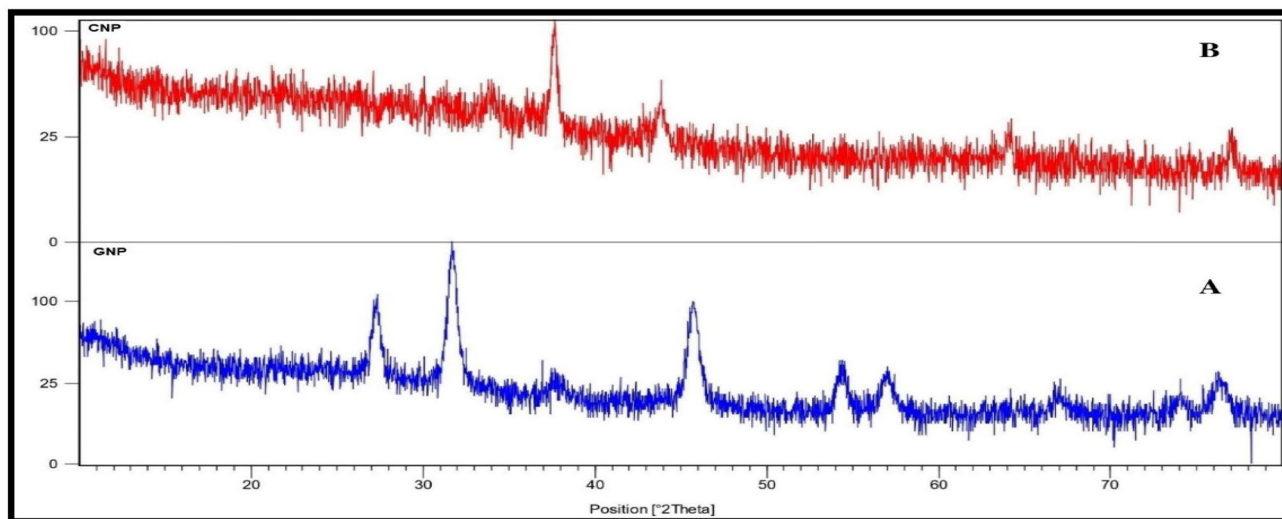


Fig. 4 Comparative XRD diffractogram of green and chemically synthesized silver nanoparticle. **A** GNP. **B** CNP

Thermal Analysis of Synthesized Silver Nanoparticles for Thermal Stability

Figure 6A, B shows the DSC-TGA curves of silver nanoparticles synthesized through green and chemically synthesized methods, respectively, through which samples' thermal stability and purity were interpreted. In the case of green synthesized AgNPs, the total weight loss was 75.98% at 80.66 °C, attributed to water and organic matter loss. After this, no weight loss was observed throughout the thermogram, which revealed the capping of silver nanoparticles by phytomolecules of fenugreek leaves. The sharp peak at 122.33°C and slight peak at 978°C are considered dehydration peaks and melting endotherm of silver, respectively, in Fig. 6A. The silver peak in Fig. 6A shows the purity of green synthesized AgNPs, which is not seen in the chemically synthesized product (Fig. 6B). In the case of chemically synthesized AgNPs, the first

weight loss (42.48%) was observed at 324.51°C, which continues up to 855.39°C, exemplifying the decomposition of particles. Ahsan et al. (2020) synthesized AgNPs using *Parthenium hysterophorus* plant extract, which was stable up to 200°C. Silver nanoparticles synthesized using *Cynara scolymus* L showed a peak at 973.42°C for metallic silver, which supports the present study [24].

X-Ray Photoelectron Spectrometer (XPS) to Confirm the Elemental Composition of Silver Nanoparticles

Figure 7A shows the XPS spectrum of green-synthesized silver nanoparticles (GNP) prepared using fenugreek leaves as a catalyst. The Ag, O, C, and N elements were detected by survey scan. The atomic concentration of C is 70.75%, N is 12.5%, O is 11.74%, sulphur is 4.12, and Ag is 0.88%. A lower concentration of Ag indicates that silver nanoparticles were protected well by phytochemical molecules in

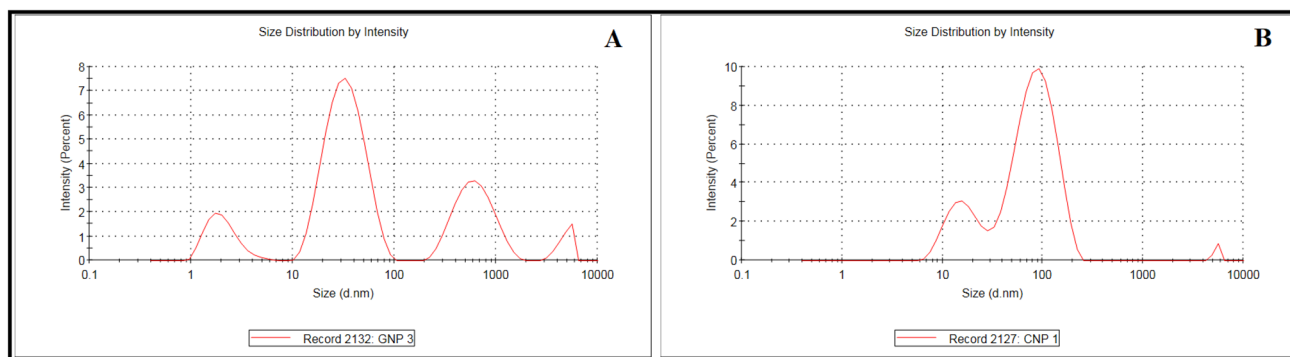


Fig. 5 Particle size analysis of green and chemically synthesized nanoparticles. **A** GNP. **B** CNP

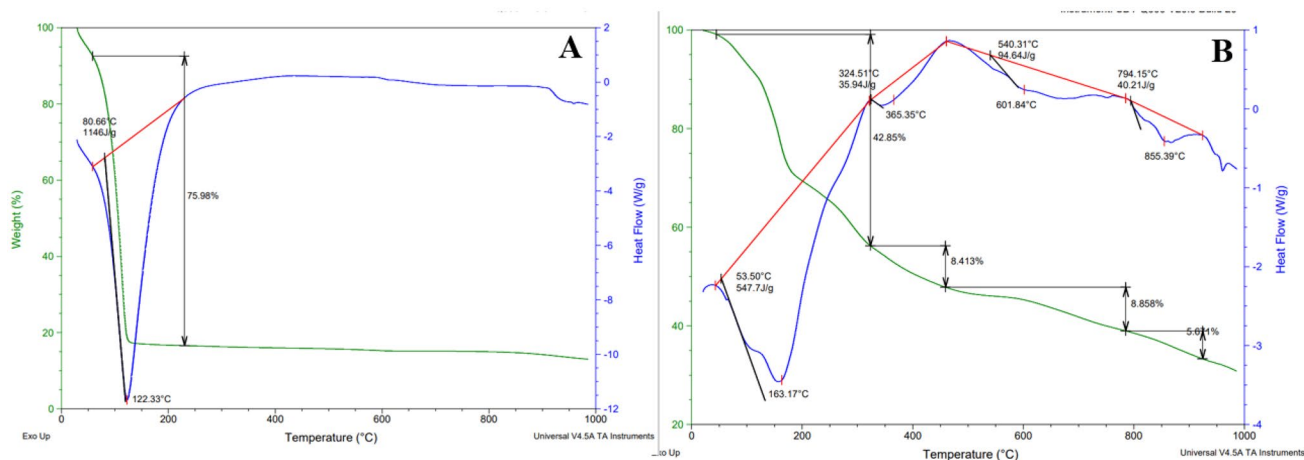


Fig. 6 Comparative thermogram of green and chemically silver nanoparticles. **A** GNP. **B** CNP

fenugreek leaves and aid in the reduction of silver toxicity. A survey scan shows a doublet peak for Ag3d, observed at 368.3 eV and 374.3 eV, corresponding to Ag 3d_{5/2} and 3d_{3/2} binding energies, respectively [25]. It shows that silver atoms synthesized by green synthesis are in pure form. Later, it might interact with electronegative elements like N or O of phytomolecules of fenugreek leaves. The evidence of a lower concentration of silver and fewer elements will benefit the toxicity free biological effects induced by AgNPs.

Figure 7B shows the XPS spectrum of chemically synthesized silver nanoparticles (CNP) prepared using sodium borohydride. The survey scan shows various elements: Na, B, Al, Mg, S, Cl, Ag, O, C, and N. The atomic concentration of Na is 0.98%, B is 2.89%, Al is 1.09%, Mg is 2.2%, S is

1.75%, Cl is 1.1%, Si is 3.1%, O is 29.59%, N is 5.89%, and C is 51.46%. The atomic percentage of Ag was not represented in the XPS result, which indicates that the chemically synthesized silver nanoparticles might have been bonded completely or might not have been reduced effectively. If it had been bonded effectively, the Ag3d spectra should show a doublet peak corresponding to Ag 3d_{5/2} and 3d_{3/2} binding energies, which is not evidenced in the spectra obtained. Instead, multiple peaks throughout the scan range were observed, indicating the synthesis of more oxidized silver nanoparticles through chemical methods instead of pure form. This oxidized form and other elements might contribute to the biological effects and toxicity of chemically synthesized AgNPs.

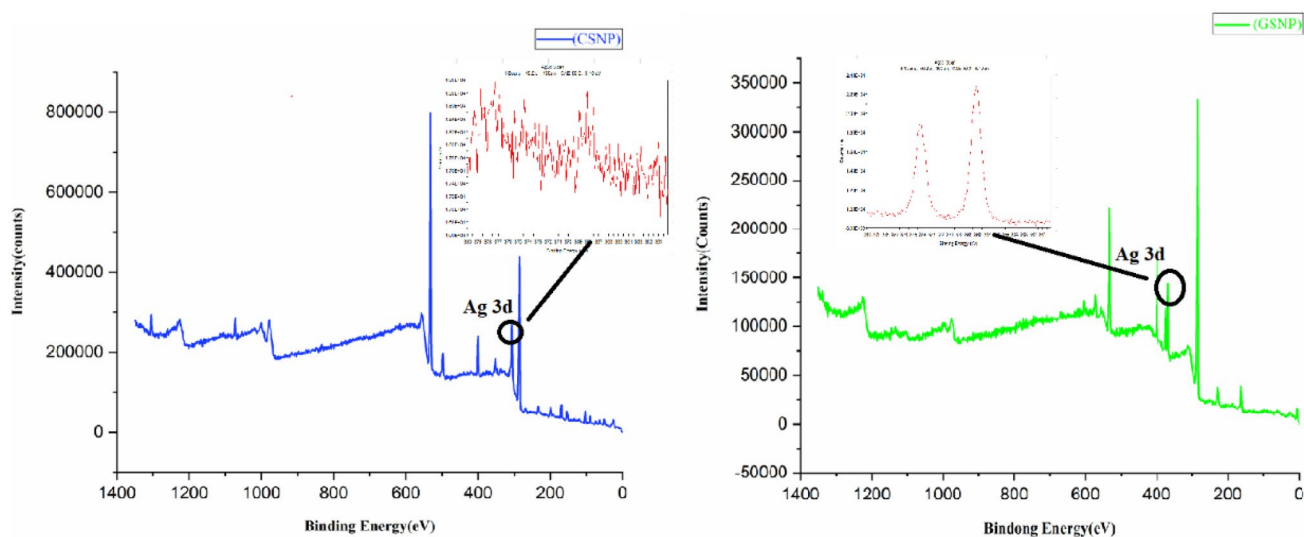


Fig. 7 X-ray photo electron spectra (XPS) of green and chemically synthesized nanoparticles

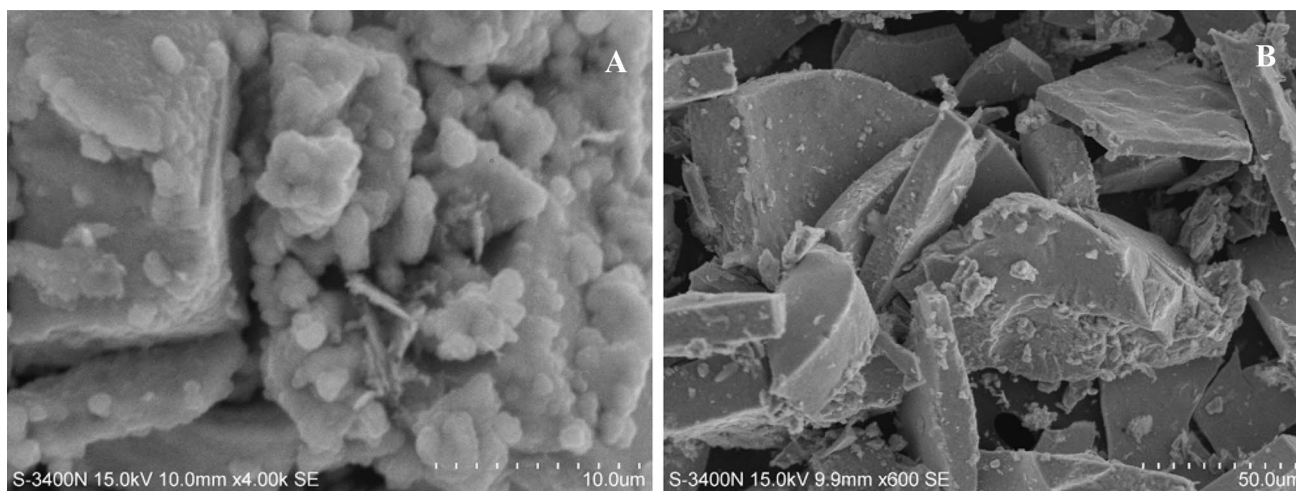


Fig. 8 Scanning electron microscopic (SEM) images of green and chemically synthesized nanoparticles. **A** GNP. **B** CNP

Morphology of Silver Nanoparticles Using Scanning Electron Microscope

Scanning electron microscopy of green synthesized nanoparticles (GNP) showed spherical-shaped particles (Fig. 8) compared to the chemically synthesized nanoparticles in different shapes. Like the current study, Meena and Chouhan et al. [26] prepared spherical-shaped silver nanoparticles using fenugreek seeds. However, in another study on silver nanoparticles synthesized using *Prosopis juliflora* leaf extracts, SEM analysis reported multiple shapes like triangles, pentagons, and hexagons [27].

Comparison of Biological Activities Exhibited by Silver Nanoparticles Synthesized by Chemical Reduction and Green Synthesis

Silver nanoparticles (AgNPs) are among the most attractive and superior nanomaterials recognized for their different applications due to their unique physicochemical properties. Accordingly, AgNPs prepared by different methods are used for biomedical applications such as antimicrobial, wound healing, bone repair, and anticancer therapy. They are also used as adjuvants in vaccines and in developing biosensors [28]. Herein, we compared the efficacy of GNP and CNP for their antioxidant, antibacterial, and wound healing potential by in vitro assay protocols.

FRAP Assay for Reducing the Power of Silver Nanoparticles

In a redox-linked colorimetric approach, the FRAP assay uses antioxidants as reductants, with the reaction mechanism depending entirely upon electron transfer. The

reducing power is given as the equivalence of ascorbic acid, which serves as a reference standard. Herein, the biologically produced AgNPs (GNP) have an IC_{50} of 29.30 mg/ml, chemically synthesized (CNP) has an IC_{50} of 3.4 mg/ml, and Vitamin C standard has the lowest IC_{50} of 0.143 mg/ml (Fig. 9). It is impressive that chemically synthesized AgNPs exhibit better free radical scavenging activity than green synthesized (GNP) due to a more oxidized form of silver nanoparticles in the CNP. In the case of GNP, the less scavenging activity is probably due to the inability of the green synthesized nanoparticles to react with the free electrons readily. As phytochemicals in the fenugreek leaf extract encapsulate the green synthesized nanoparticles, they might not react with free electrons. Although the reducing potential of GNP is not on par with the CNP, the activity is probably after sustained release from the biogenic base. This mechanism is safe and may result in lesser toxicity when compared to the chemically synthesized AgNPs, which are readily exposed and oxidized.

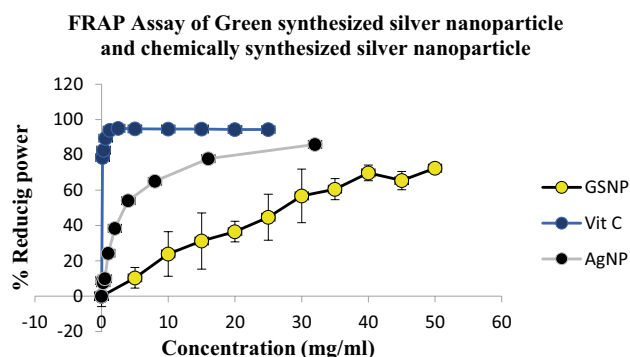
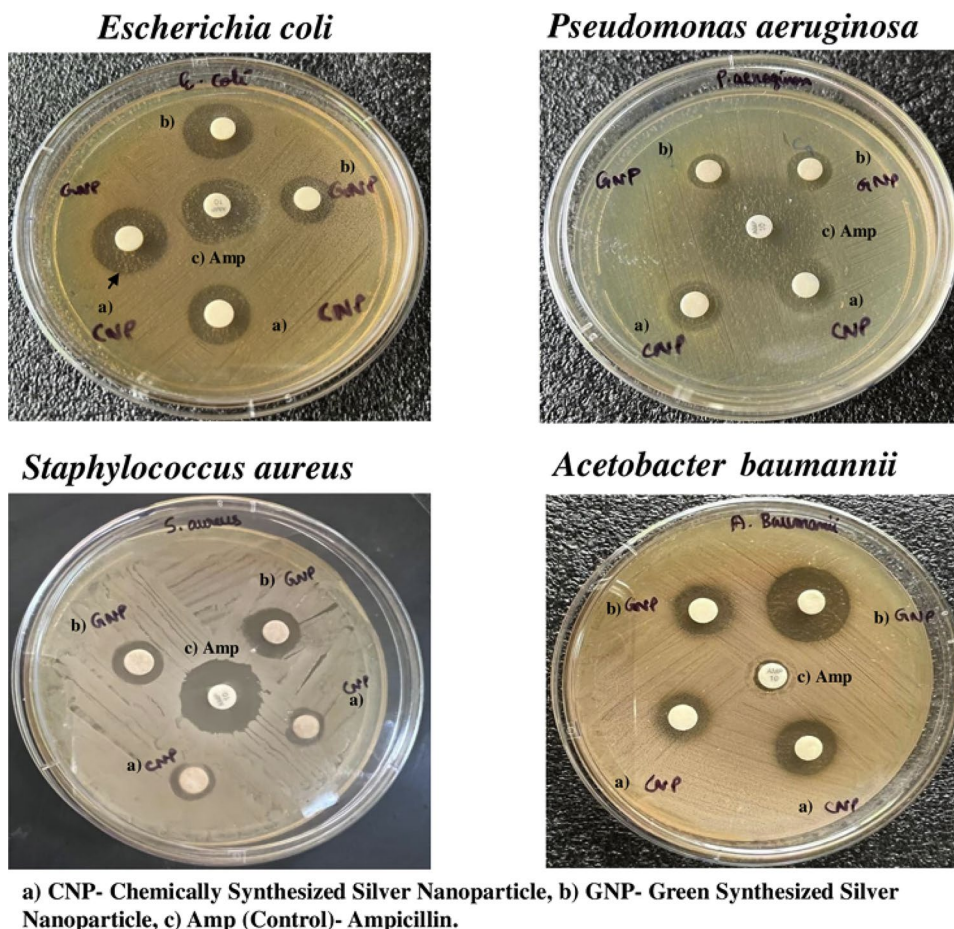


Fig. 9 Ferric reducing antioxidant power (FRAP) of green and chemically synthesized nanoparticles

Fig. 10 Antimicrobial activity of green and chemically synthesized silver nanoparticles



Antimicrobial Activity of Silver Nanoparticles by Disc Diffusion Method

The antibacterial activities of GNP and CNP were evaluated using the disc diffusion method and were compared with the positive control Ampicillin (10 µg/disc). Figure 10 and Table 1 show that GNP showed more inhibition zone than CNP. Though both the nanoparticles showed activities against all four microorganisms, biogenic silver nanoparticles showed a higher zone of inhibition against *E. coli*. The results of the present study are in congruence with

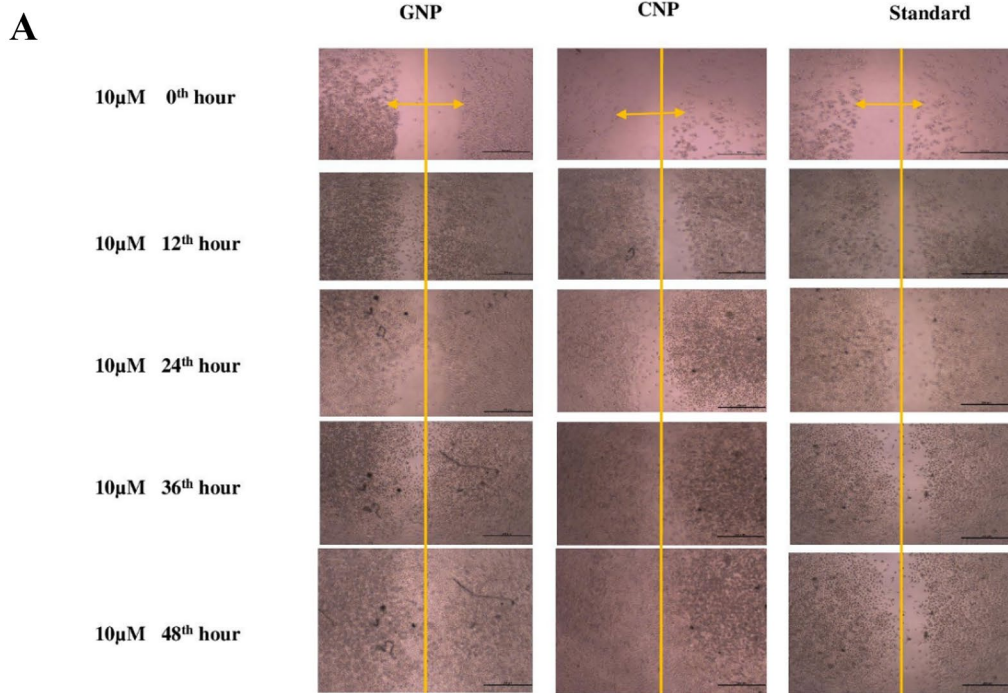
the study reported by G. Ghoshal and M. Singh [23]. They reported more zone of inhibition of green synthesized nanoparticles using fenugreek leaves against *E. coli*.

Moreover, they reported less zone of inhibition for *S. aureus*, but in our study, the zone of inhibition against *S. aureus* and *E. coli* for biogenic silver nanoparticles was almost similar. It is worth mentioning that the potency of silver nanoparticles' antimicrobial activity depends on the nanoparticle's size and shape [29]. Notably, GNP is spherical, exhibiting better antimicrobial activity compared to CNP, evidenced in the (Fig. 7) SEM micrographs.

Table 1 Antimicrobial activity of green and chemically synthesized silver nanoparticle

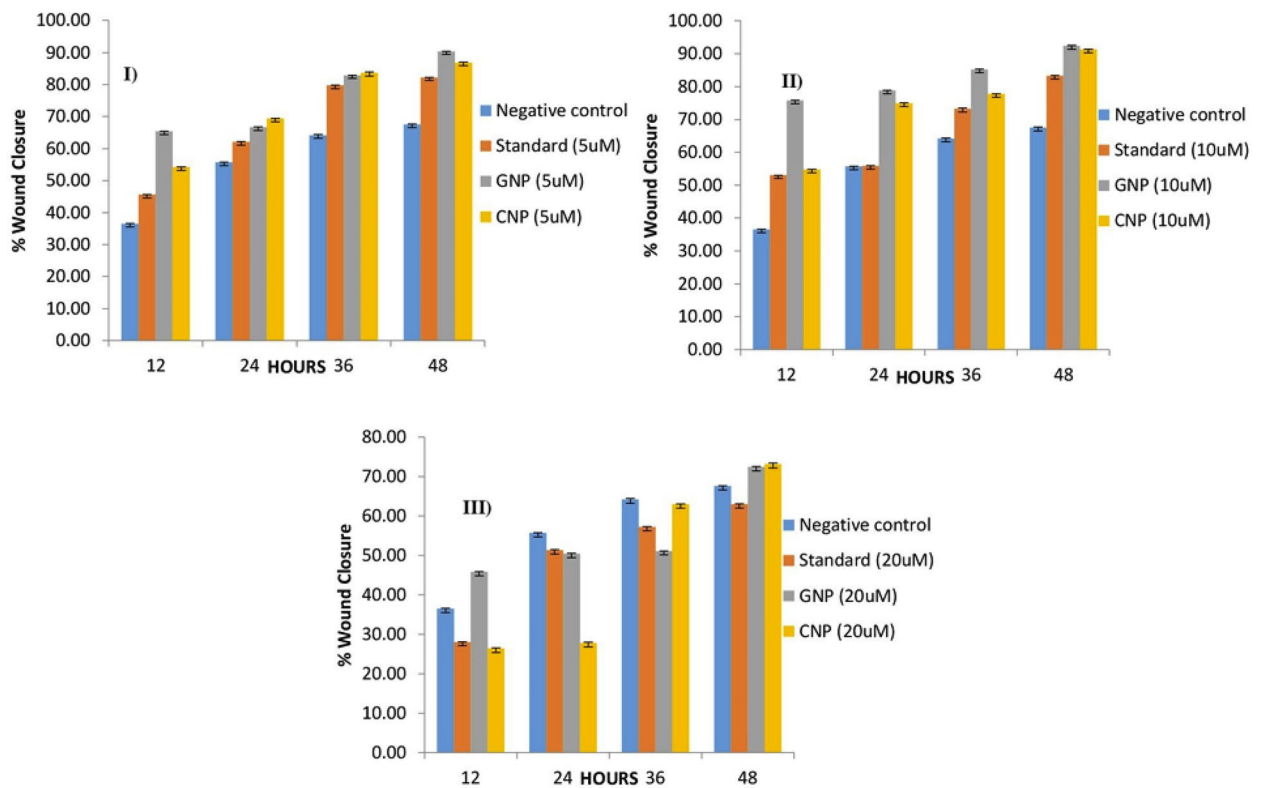
Compound/disc potency	Zone of inhibition (mm)			
	<i>Escherichia coli</i>	<i>Acetobacter baumannii</i>	<i>Pseudomonas aeruginosa</i>	<i>Staphylococcus aureus</i>
Ampicillin (control, 10 µg)	14 ±1.7	20.7 ±1.2	24.7 ±0.6	17 ±2.6
Silver nanoparticle by green synthesis (GNP) (3 mg/ml)	12 ±0.0	12 ±0.0	11.7 ±0.6	12 ±0.0
Silver nanoparticle by green synthesis (GNP) (4 mg/ml)	13.7 ±0.6	13 ±0.0	12.7 ±0.6	13 ±0.0
Silver nanoparticle by chemical synthesis (CNP) (3 mg/ml)	12 ±0.0	11.7 ±0.6	11 ±0.0	11 ±0.0
Silver nanoparticle by chemical synthesis (CNP) (4 mg/ml)	12.3 ±0.6	12 ±0.0	11.7 ±0.6	12 ±0.0

*The values represent the average of two determinations ± standard deviations. Ampicillin (10 µg/disc) was used as the positive control



Migration of GNP (Green Synthesized Nanoparticle) and CNP (Chemically Synthesized Nanoparticle) compared with Silver Nitrate Gel (Standard) on L929 fibroblast cells after scratch induction. Scale Bar =200 μ m.

B



Percentage of Wound Closure Analysis by Scratch Assay. (I) 5 μ m, (II) 10 μ m, and (III) 20 μ m concentration of GNP (Green Synthesized Silver Nanoparticle), CNP (Chemically Synthesized Silver Nanoparticle), and Standard (Silver Nitrate Gel). Data represented are mean \pm of SEM values.

Fig. 11 A Analysis of cellular migration by in vitro scratch assay. B Percentage of wound closure analysis by scratch assay

In Vitro Cell Viability and Wound Healing Activity of Silver Nanoparticles

MTT Assay The cell viability of AgNPs synthesized using biological and chemical approaches was determined by MTT assay on L929 fibroblast cells. The IC_{50} concentration of green synthesized nanoparticles is $9.558 \mu\text{M}$ compared to $9.065 \mu\text{M}$ by chemically synthesized nanoparticles; Varghese et al. (2019) reported 6.25 and $12.5 \mu\text{g/ml}$ as IC_{50} values for green synthesized silver nanoparticles using Fenugreek when added to MCF7 and Vero cells, respectively [30]. The author also concluded less toxicity with this dose than in the other reported literature. In our study, the IC_{50} value for both GNP and CNP is near $9 \mu\text{M}$ (equivalent to $2 \mu\text{g/ml}$), which is considered minimal and would have safe applications. It is confirmed through several studies that the size of the AgNP mediates cell responses, including uptake, cytotoxicity, ability to penetrate biological barriers, and ROS generation. Likewise, spherical Ag nanoparticles have negligible effects on cells [31]. In the present study, GNP synthesized is spherical, which probably mediates the dose-dependent cell viability.

Scratch Assay The use of silver in wound healing dates back to ancient times. The comparison of the wound-healing potential of the silver nanoparticles prepared chemically and biologically was checked using the scratch assay on fibroblast cells. The scratch assay is a simple and versatile method to measure wound healing, as cell migration is crucial for wound healing [32]. Furthermore, silver nanoparticles can also drive the differentiation of fibroblasts into myofibroblasts, promoting wound contraction [33]. Based on the IC_{50} value obtained from the MTT assay, which is around 9 to $10 \mu\text{M}$, the scratch assay was performed at three doses (5, 10, $20 \mu\text{M}$) (Fig. 11A, B). The treatment of L929 fibroblast cells with $10 \mu\text{M}$ of chemically and green synthesized AgNP improved the proliferation of the cells through migration. The migration of L929 fibroblast cells was dramatically reduced at $20 \mu\text{M}$ on both AgNP treatments compared to $5 \mu\text{M}$ of the nanoparticle-treated L929 fibroblast cells. This is possible because cell death was observed at a dose of $20 \mu\text{M}$. In comparison between green and chemically synthesized AgNPs with $10 \mu\text{M}$ dose, the green synthesized AgNPs showed better cell migration, confirming faster wound healing with negligible toxicity. Phytomolecules such as flavonoids, alkaloids, and coumarins in fenugreek leaves present on the surface of biologically synthesized nanoparticles possess inherent biological activities like anti-inflammatory, antioxidant, and wound-healing properties. In the case of wound healing, the enhanced cellular migration induced by biologically synthesized nanoparticles compared to the chemically synthesized nanoparticles is possibly due

to the synergistic effect of the phytomolecules in fenugreek leaves. Hence, the improved wound-healing response was observed in biogenic nanosilver in our study.

The reduced toxicity may be attributed to the larger size of GNP over CNP, as evidenced by the XRD data.

Conclusion

With several concerns about the toxicity of nanomaterials, the present study was carried out to identify the safety and efficacy of the green synthesized nanoparticle over the chemically synthesized AgNP. It is identified that the green synthesized nanoparticle is larger than the chemically synthesized nanoparticle by interpreting various characterization data such as UV-visible spectroscopy, spectrofluorometry, and XRD. Furthermore, the FTIR analysis confirmed the formation of silver nanoparticles. Interestingly, the green synthesized nanoparticles are more stable and crystalline than chemically synthesized nanoparticles, which were established through thermal analysis and X-ray diffraction data. XPS data attested that the phytochemicals in fenugreek leaves used for the green synthesis of AgNPs act as reducing and capping agents. Phytomolecules in fenugreek leaves facilitate the reduction process of silver ions (Ag^+) to silver nanoparticles (Ag^0 or Ag^-) which have zero oxidation state or negative charge. This conversion reduces the toxicity of silver nanoparticles compared to the metallic silver. Moreover, the phytomolecules in fenugreek leaves provides stability by inhibiting the aggregation and agglomeration of the formed silver nanoparticles. However, in the case of chemically synthesized nanoparticles, the sodium borohydride acts only as the reducing agent but not as a capping agent, and the reduction of toxicity of silver nanoparticles is not warranted. The presence of Ag^+ and its encapsulation by the phytochemicals in fenugreek leaf extract in the green synthesis of AgNPs was confirmed by XPS data.

In general, biologically synthesized silver nanoparticles have good biocompatibility compared to chemically synthesized ones. The presence of phytomolecules such as flavonoids, alkaloids, and coumarins in fenugreek leaves on the surface of silver can reduce silver toxicity which aids in the biocompatibility leading to good biological effects and making them suitable for many biomedical applications. Regarding the reducing power of AgNP identified through FRAP assay, the IC_{50} value of the green synthesized nanoparticle is comparatively higher than the chemically synthesized nanoparticle. This difference is probably due to phytochemicals as capping agents in the green synthesized nanoparticles, wherein the silver is not readily

exposed. The higher IC₅₀ value indirectly reveals the safe use of biologically synthesized silver nanoparticles compared to the chemically synthesized one. The cell viability of the chemically and green synthesized nanoparticle is almost similar. Still, the green synthesized nanoparticle shows better cell migration and wound-healing ability as evaluated by scratch assay. Therefore, from the above data, green synthesized nanoparticle is preferred over chemically synthesized nanoparticles as they are non-toxic and possibly does not exhibit negative environmental and health impacts. Further studies are warranted to develop the biogenic silver nanoparticles as potent dosage forms for new antibacterial, anticancer, or antifungal agents in the near future.

Acknowledgements The authors acknowledge the DBT, DHR, RGNF, and UGC fellowship, respectively from Govt. of India to execute this research work. The DST (FIST and UGC (SAP) grants to the Department of Biotechnology and the Central Instrumentational Facility of Pondicherry University for Infrastructural facilities are acknowledged.

Author Contribution PP: investigation and methodology; NS: conceptualization, validation, formal analysis, and writing—original draft; K K: investigation, methodology, and formal analysis; SR: investigation and methodology; HRV: data curation, writing—review and editing and supervision.

Data Availability The data and materials will be made available on request to the authors.

Declarations

Ethics Approval Not applicable.

Consent to Participate and Publish All authors give consent to participate and publish.

Conflict of Interest The authors declare no conflict of interests.

References

- Kaviya S, Santhanalakshmi J, Viswanathan B. Green synthesis of silver nanoparticles using *Polyalthia longifolia* leaf extract along with D-sorbitol: study of antibacterial activity. *J Nanotechnol.* 2011;2011.
- Laurent S, et al. Magnetic iron oxide nanoparticles: synthesis, stabilization, vectorization, physicochemical characterizations, and biological applications. *Chem Rev.* 2008;108(6):2064–110.
- Crabtree JH, Burchette RJ, Siddiqi RA, Huen IT, Hadnott LL, Fishman A. The efficacy of silver-ion implanted catheters in reducing peritoneal dialysis-related infections. *Perit Dial Int.* 2003;23(4):368–374.
- De Gaetano F, Ambrosio L, Raucci MG, Marotta A, Catauro M. Sol-gel processing of drug delivery materials and release kinetics. *J Mater Sci Mater Med.* 2005;16(3):261–265.
- Tang S, Mao C, Liu Y, Kelly DQ, Banerjee SK. Protein-mediated nanocrystal assembly for flash memory fabrication. *IEEE Trans Electron Devices.* 2007;54(3):433–8.
- Narayanan KB, Sakthivel N. Green synthesis of biogenic metal nanoparticles by terrestrial and aquatic phototrophic and heterotrophic eukaryotes and biocompatible agents. *Adv Colloid Interface Sci.* 2011;169(2):59–79.
- Iravani S, Zolfaghari B. Green synthesis of silver nanoparticles using *Pinus eldarica* bark extract. *Biomed Res Int.* 2013;2013.
- Mittal AK, Chisti Y, Banerjee UC. Synthesis of metallic nanoparticles using plant extracts. *Biotechnol Adv.* 2013;31(2):346–56.
- Das RK, Gogoi N, Bora U. Green synthesis of gold nanoparticles using *Nyctanthes arbortristis* flower extract. *Bioprocess Biosyst Eng.* 2011;34(5):615–9.
- Wani SA, Kumar P. Fenugreek: a review on its nutraceutical properties and utilization in various food products. *J Saudi Soc Agric Sci.* 2018;17(2):97–106.
- Kishore K, Selvasudha N, Vasanthi HR. The multifaceted role of pectin in keratin based nanocomposite with antimicrobial and antioxidant activity. *J Drug Deliv Sci Technol.* 2022;75: 103661.
- Luu T, Cao XT, Nguyen V, Pham NL, Nguyen HL, Nguyen CT. Simple controlling eco-friendly synthesis of silver nanoparticles at room temperature using lemon juice extract and commercial rice vinegar. *J Nanotechnol.* 2020;2020.
- Umashankari J, Inbakandan D, Ajithkumar TT, Balasubramanian T. Mangrove plant, *Rhizophora mucronata* (Lamk, 1804) mediated one pot green synthesis of silver nanoparticles and its antibacterial activity against aquatic pathogens. *Aquat Biosyst.* 2012;8(1):1–7.
- Rizwana H, Alwhibi MS, Aldarone HA, Awad MA, Soliman DA, Bhat RS. Green synthesis, characterization, and antimicrobial activity of silver nanoparticles prepared using *Trigonella foenum-graecum* L. leaves grown in Saudi Arabia. *Green Process Synth.* 2021;10(1):421–9.
- Pandey JK, et al. Silver nanoparticles synthesized by pulsed laser ablation: as a potent antibacterial agent for human enteropathogenic gram-positive and gram-negative bacterial strains. *Appl Biochem Biotechnol.* 2014;174(3):1021–1031.
- Quintero-Quiroz C, et al. Optimization of silver nanoparticle synthesis by chemical reduction and evaluation of its antimicrobial and toxic activity. *Biomater Res.* 2019;23(1):1–15.
- Melkamu WW, Bitew LT. Green synthesis of silver nanoparticles using *Hagenia abyssinica* (Bruce) JF Gmel plant leaf extract and their antibacterial and antioxidant activities. *Heliyon.* 2021;7(11):e08459.
- Alwhibi MS, Soliman DA, Awad MA, Rizwana H, Marraiki NA. Biosynthesis of silver nanoparticles using fenugreek seed extract and evaluation of their antifungal and antibacterial activities. *J Comput Theor Nanosci.* 2018;15(4):1255–60.
- Parang Z, Keshavarz A, Farahi S, Elahi SM, Ghoranneviss M, Parhoodeh S. Fluorescence emission spectra of silver and silver/cobalt nanoparticles. *Sci Iran.* 2012;19(3):943–7.
- Shang M, et al. Studies on flavonoids from fenugreek (*Trigonella foenum-graecum* L.), *Zhongguo Zhong yao za zhi= Zhongguo zhong-yao zazhi= China. J Chinese Mater Medica.* 1998;23(10):614–616.
- Avalos-Soriano A, De la Cruz-Cordero R, Rosado JL, Garcia-Gasca T. 4-Hydroxyisoleucine from fenugreek (*Trigonella foenum-graecum*): effects on insulin resistance associated with obesity. *Molecules.* 2016;21(11):1596.
- Thiruvengadam V, Bansod AV. Characterization of silver nanoparticles synthesized using chemical method and its antibacterial property. *Biointerface Res Appl Chem.* 2020;10:7257–7264.
- Ghoshal G, Singh M. Characterization of silver nanoparticles synthesized using fenugreek leaf extract and its antibacterial activity. *Mater Sci Energy Technol.* 2022;5:22–29.
- Sampaio S, Viana JC. Production of silver nanoparticles by green synthesis using artichoke (*Cynara scolymus* L.) aqueous extract and measurement of their electrical conductivity. *Adv Nat Sci Nanosci Nanotechnol.* 2018;9(4):45002.

25. Porcaro F, et al. Synthesis and structural characterization of silver nanoparticles stabilized with 3-mercapto-1-propanesulfonate and 1-thiogluco-1-thiol mixed thiols for antibacterial applications. *Materials (Basel)*. 2016;9(12):1028.
26. Meena RK, Chouhan N. Biosynthesis of silver nanoparticles from plant (fenugreek seeds) reducing method and their optical properties. *Res J Recent Sci ISSN*. 2015;2277:2502.
27. Raja K, Saravanakumar A, Vijayakumar R. “Efficient synthesis of silver nanoparticles from *Prosopis juliflora* leaf extract and its antimicrobial activity using sewage”, *Spectrochim. Acta Part A Mol Biomol Spectrosc*. 2012;97:490–4.
28. Xu L, Yi-Yi W, Huang J, Chun-Yuan C, Zhen-Xing W, Xie H. Silver nanoparticles: synthesis, medical applications and biosafety. *Theranostics*. 2020;10(20):8996.
29. Cheon JY, Kim SJ, Rhee YH, Kwon OH, Park WH. Shape-dependent antimicrobial activities of silver nanoparticles. *Int J Nanomedicine*. 2019;14:2773.
30. Varghese R, Almalki MA, Ilavenil S, Rebecca J, Choi KC. Silver nanoparticles synthesized using the seed extract of *Trigonella foenum-graecum* L. and their antimicrobial mechanism and anticancer properties. *Saudi J Biol Sci*. 2019;26(1):148–54.
31. Hernández-Sierra JF, Galicia-Cruz O, Salinas-Acosta A, Ruíz F, Piedant-Pérez M, Pozos-Guillén A. In vitro cytotoxicity of silver nanoparticles on human periodontal fibroblasts. *J Clin Pediatr Dent*. 2011;36(1):37–42.
32. Martinotti S, Ranzato E. Scratch wound healing assay, in *Epidermal cells*, Springer. 2019;225–229.
33. Paladini F, Pollini M. Antimicrobial silver nanoparticles for wound healing application: progress and future trends. *Materials (Basel)*. 2019;12(16):2540.

Publisher's Note Springer Nature remains neutral with regard to jurisdictional claims in published maps and institutional affiliations.

Springer Nature or its licensor (e.g. a society or other partner) holds exclusive rights to this article under a publishing agreement with the author(s) or other rightsholder(s); author self-archiving of the accepted manuscript version of this article is solely governed by the terms of such publishing agreement and applicable law.